THE JOURNAL OF BIOLOGICAL CHEMISTRY
Vol. 277, No. 12, Issue of March 22, pp. 10642–10646, 2002

Printed in U.S.A.

Crystal Structure of Human L-Isoaspartyl Methyltransferase*

Received for publication, January 9, 2002, and in revised form, January 14, 2002
Published, JBC Papers in Press, January 15, 2002, DOI 10.1074/jbc.M200229200

Carsten Ryttersgaard‡§, Scott C. Griffith‡, Michael R. Sawaya§, Duncan C. MacLaren‡, Steven Clarke‡, and Todd O. Yeates‡§¶

From the ‡Department of Chemistry and Biochemistry and Molecular Biology Institute, §UCLA-DOE Laboratory of Structural Biology and Molecular Medicine, University of California, Los Angeles, California 90095-1569

The enzyme L-isoaspartyl methyltransferase initiates the repair of damaged proteins by recognizing and methylating isomerized and racemized aspartyl residues in aging proteins. The crystal structure of the human enzyme containing a bound *S*-adenosyl-L-homocysteine cofactor is reported here at a resolution of 2.1 Å. A comparison of the human enzyme to homologs from two other species reveals several significant differences among otherwise similar structures. In all three structures, we find that three conserved charged residues are buried in the protein interior near the active site. Electrostatics calculations suggest that these buried charges might make significant contributions to the energetics of binding the charged *S*-adenosyl-L-methionine cofactor and to catalysis. We suggest a possible structural explanation for the observed differences in reactivity toward the structurally similar L-isoaspartyl and D-aspartyl residues in the human, archael, and eubacterial enzymes. Finally, the human structure reveals that the known genetic polymorphism at residue 119 (Val/Ile) maps to an exposed region away from the active site.

The loss of biological functions in the aging process can be attributed in part to nonenzymatic chemical reactions that degrade biomolecules including DNA, proteins, and small molecules. We have been interested in enzymatic mechanisms from which organisms have evolved to limit the accumulation of isomerized and racemized aspartyl residues, which form spontaneously from normal L-aspartic acid and L-asparagine residues within proteins as they age. Much attention has been directed at understanding the action of the L-isoaspartate(D-aspartate) *O*-methyltransferase or protein L-isoaspartyl methyltransferase (PIMT)[1] (EC 2.1.1.77). PIMT is an enzyme that recognizes altered aspartyl residues in proteins and polypeptides and drives their eventual conversion to normal L-aspartyl residues (1–3). In the best-characterized pathway, a methyl group is transferred from *S*-adenosyl-L-methionine (AdoMet) to form a methyl ester on the α-carboxyl group of an L-isoaspartyl residue. Subsequent nonenzymatic reactions result in rapid L-succinimide formation and hydrolysis, which generates some "repaired" L-aspartyl residues as well as some L-isoaspartyl residues, which can then enter the cycle again for eventual conversion to the normal peptide linkage. PIMTs have been highly conserved during evolution and are found in almost all eucaryotic cells as well as in most archaebacteria and most Gram-negative eubacteria (4, 5).

Recently, three-dimensional structures have been determined for PIMT from the hyperthermophilic eubacterium *Thermotoga maritima* (6) and the thermophilic archaebacterium *Pyrococcus furiosus* (7). With the exception of a C-terminal domain apparently unique to the *T. maritima* enzyme, these enzymes have similar amino acid sequences and a similar three-dimensional fold (5). For the *P. furiosus* enzyme, the crystal structures of AdoMet-liganded and isoaspartyl peptide-liganded forms have revealed how the enzyme can recognize a wide variety of damaged L-isoaspartyl and D-aspartyl residues while excluding normal L-aspartyl residues (7). However, despite their sequence similarities, the kinetic properties and substrate specificities of the enzymes from various species are distinct. For example, the *T. maritima* enzyme is unable to methylate polypeptides containing D-aspartyl residues (5), whereas the *P. furiosus* enzyme is able to recognize such racemized residues (8).

With an interest in mammalian aging, efforts have been focused on understanding the three-dimensional structure and substrate specificity of the human form of the enzyme. A particularly interesting puzzle is why the human and *P. furiosus* enzymes have the ability to also repair methylated D-aspartyl residues and why these enzymes also appear to have a considerably higher affinity for L-isoaspartyl residues than do many plant and eubacterial enzymes (9). The human enzyme is produced in two alternatively spliced forms that have distinct C termini (10, 11). There is also a widespread genetic polymorphism that results in the presence of either a valine or isoleucine residue at position 119 (12).

EXPERIMENTAL PROCEDURES

Data Collection and Processing—The human PIMT was cloned, expressed, and purified (13), and subsequent crystallization screenings were performed in the presence of an acidic solution that was saturated with respect to dithiothreitol and AdoHcy as described previously (14–16). The best crystals were grown from a solution of 0.2 M MgAc, 0.1 M cacodylate, pH 6.5, and 20% polyethylene glycol 8000. Data were collected in 1° oscillations using one cryo-cooled crystal at beamline X8C at the National Synchrotron Light Source. A data set was collected to 2.1-Å resolution and processed using DENZO and SCALEPACK (17). The crystal belongs to the monoclinic space group $P2_1$ with $a = 48.0$ Å, $b = 53.7$ Å, $c = 49.0$ Å, $\beta = 115.6°$, and one molecule in the asymmetric unit. In the initial data processing, an ice-ring caused many reflections to be discarded, resulting in an acceptable value for R_{sym} (5.3%) but poor

* This work was supported in part by the Department of Energy Grant DE-FC03-87ER60615 (to T. O. Y.) and National Institutes of Health Grants AG18000 and GM26020 (to S. C.). The costs of publication of this article were defrayed in part by the payment of page charges. This article must therefore be hereby marked "*advertisement*" in accordance with 18 U.S.C. Section 1734 solely to indicate this fact.

The atomic coordinates and structure factors (code 1KR5) have been deposited in the Protein Data Bank, Research Collaboratory for Structural Bioinformatics, Rutgers University, New Brunswick, NJ (http://www.rcsb.org/).

¶ To whom correspondence should be addressed: Dept. of Chemistry and Biochemistry and Molecular Biology Institute, UCLA-DOE Laboratory of Structural Biology and Molecular Medicine, Box 951569, Los Angeles, CA 90095-1569. Tel.: 310-206-4866; Fax: 310-206-3914; E-mail: yeates@mbi.ucla.edu.

[1] The abbreviations used are: PIMT, protein L-isoaspartyl methyltransferase; AdoHcy, *S*-adenosyl-L-homocysteine; AdoMet, *S*-adenosyl-L-methionine; K_BT, Boltzman constant times temperature.

coverage (completeness = 82.5%). This incompleteness hindered structure determination. By reintegrating the data with a higher threshold for background noise, the number of reflections increased from 10,970 to 12,512, and the completeness and R_{sym} were increased to 94.7 and 7.4% overall. In the outermost resolution shell, the corresponding values were 75.0 and 25.6%.

TABLE I
Diffraction and refinement data

Parameters	Values
Unit cell dimensions	
a, *b*, *c* (Å)	48.0, 53.7, 49.0
β (°)	115.6
Space group	$P2_1$
No. of reflections measured	47,131
No. of unique reflections	12,501
Resolution range (Å)	44.2–2.1
Completeness[a] (%)	94.7 (75.0)
R_{merge}[a,b] (%)	7.4 (25.6)
Refinement	
R_{work}, R_{free}[c] (%)	22.1, 26.4
No. of nonhydrogen protein atoms	1648
No. of nonhydrogen atoms in cofactor	26
No. of water molecules	64
Average B-factor (Å^2)	
All nonhydrogen atoms	46.1
Protein atoms	46.0
AdoHcy	38.9
Water	50.1
Residues with double conformations	Met-63, Glu-113, Arg-123
Root mean square values from ideality	
Bond lengths (Å)	0.007
Bond angles (°)	1.4
Dihedral angles (°)	23.8

[a] Values shown in parentheses correspond to the high resolution shell.
[b] $R_{merge} = \Sigma_{hkl}\Sigma_i|I(hkl)_i - \langle I(hkl)\rangle|/\Sigma_{hkl}\Sigma_i I(hkl)_i$.
[c] $R_{work} = \Sigma||F_o(hkl)| - k|F_c(hkl)||/\Sigma|F_o(hkl)|$. R_{free} is calculated for a "test" set of reflections that were not included in the refinement.

Structure Solution and Refinement—The structure was solved by molecular replacement with the program EPMR (18) using the structure of PIMT from *P. furiosus* (7) as a search model (Protein Data Bank accession number 1JG1). In the resulting $2F_o - F_c$ electron density map, an atomic model was easily built and adjusted using the program O (19). The structure was refined by simulated annealing and B-factor refinement as implemented in the program CNS (20). After three rounds of model building and refinement, water molecules were inserted into the model, and the refinement was converged after an additional three cycles. The final model contains residues 7–224, *S*-adenosyl-L-homocysteine, and 64 water molecules. The stereochemistry was verified with the programs PROCHECK (21) and ERRAT (22). The final *R* value is 22.3% (R_{free} = 26.4%) (Table I).

Electrostatics Calculations—The electrostatic potential in the region of space encompassing the protein molecule was calculated by solving the Poisson-Boltzmann equation on a three-dimensional grid as described by Warwicker and Watson (23) and implemented by others (24, 25) using locally written software. The grid spacing was 0.75 Å. The solvent and protein regions were assigned dielectric values of 78 and 4, respectively, and the Debye constant was taken to be 0.128 Å^{-1}. Asp, Glu, Arg, and Lys residues were assigned their full charges. The linear finite difference equations were solved by iteration using simultaneous overrelaxation and Chebyshev acceleration (26). The values for the resulting electrostatic potential at particular points of interest were obtained by trilinear interpolation on the grid.

RESULTS AND DISCUSSION

Protein Fold—The human PIMT enzyme folds as a doubly wound $\alpha/\beta/\alpha$ sandwich structure as expected for this superfamily of enzymes (27, 28). As recently reported in the structures from *T. maritima* (6) and *P. furiosus* (7), β-strands 6 and 7 are rearranged relative to the classical Rossman fold in what is now a familiar trademark of the PIMT enzymes. The labeling of secondary structural elements is shown in Fig. 1*A* illustrating the central $\alpha/\beta/\alpha$ motif along with additional N-terminal α-hel-

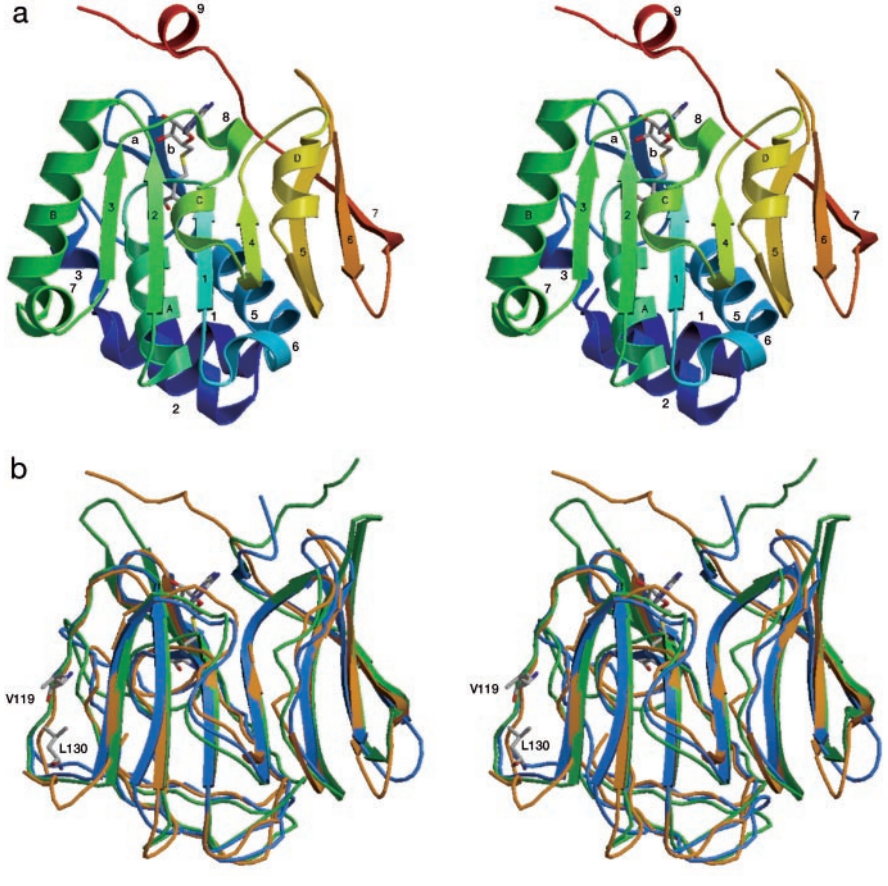

FIG. 1. *a*, stereoview of the overall fold of human PIMT. Secondary structure elements in the characteristic $\alpha/\beta/\alpha$ doubly wound fold have been labeled in agreement with earlier studies. Additional α-helices have been numbered consecutively in agreement with Skinner *et al.* (6) and Griffith *et al.* (7). The AdoHcy cofactor is shown as a stick model. *b*, a structural comparison of human PIMT structure described in this work and structures from *T. maritima* (6) and *P. furiosus*. The human structure is shown in *orange*, the *P. furiosus* structure (1JG3) is blue, and the *T. maritima* structure is green. For clarity, the N-terminal domain in the *T. maritima* structure is not shown. The AdoHcy cofactor and the Val-119 and Leu-130 residues highlighted in Fig. 2*c* from human PIMT are shown in stick models. All figures were made with Molscript (30) and Raster3D (31).

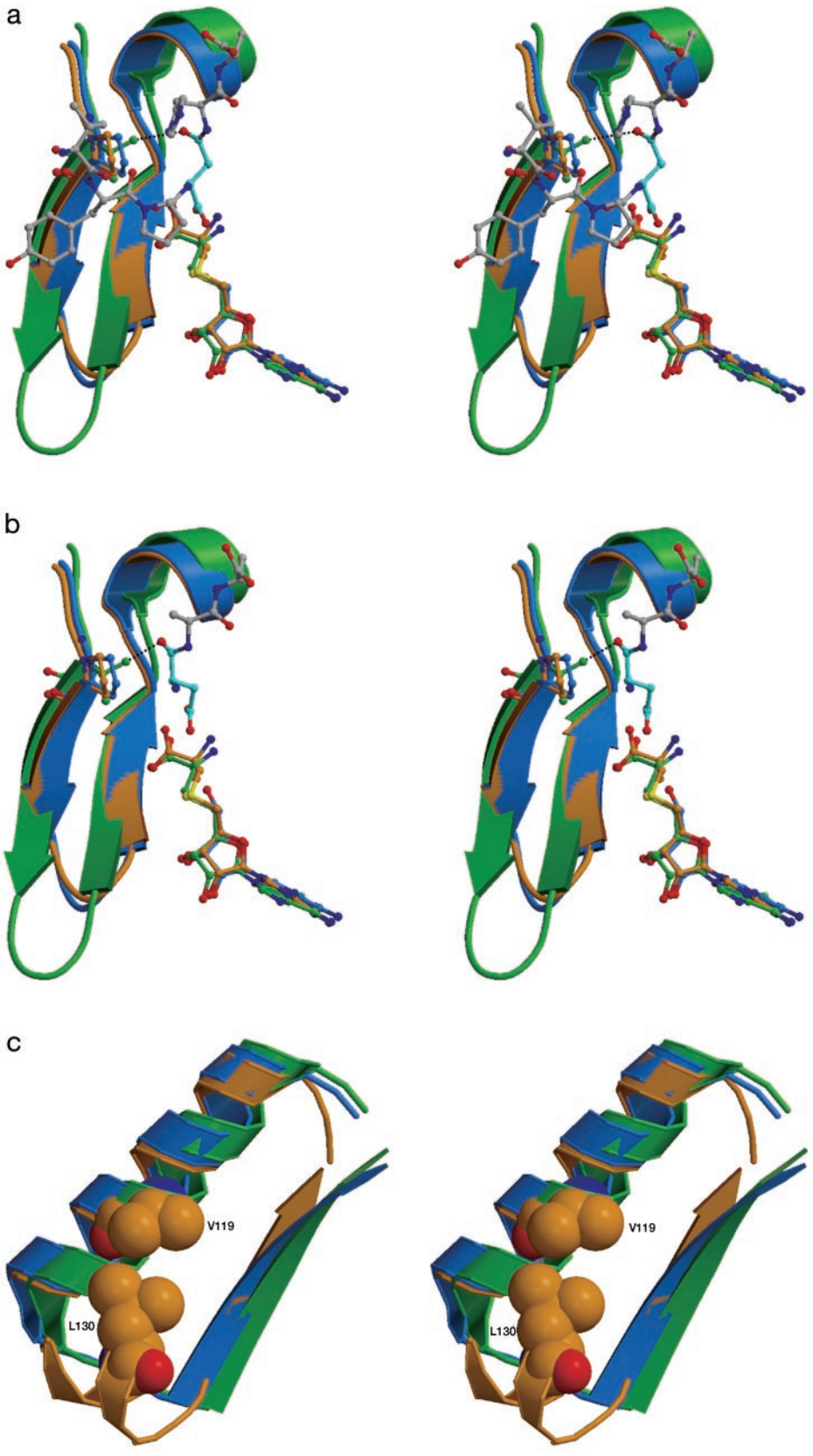

FIG. 2. *a*, a critical part of the PIMT substrate binding site. The VYP(L-isoAsp)HA peptide, present in the *P. furiosus* structure (1JG3), is shown in *cyan* (L-isoAsp) and *gray*. The human, *P. furiosus,* and *T. maritima* structures are color coded as in Fig. 1*b*. The conserved proline, Pro-49 in human and Pro-65 in *P. furiosus*, is replaced by a valine (Val-45) in the *T. maritima* structure. The *dashed line* marks the distance (3.1 Å) between CG2 in Val-45 from *T. maritima* and the carbonyl oxygen in L-isoAsp from the *P. furiosus* structure. The L-isoAsp substrate clearly fits into the active site of the structure from all three species. *b*, for contrast, the AA(D-Asp) peptide (*gray* and *cyan*) is shown in the conformation obtained by docking it into the *P. furiosus* structure using Autodock as described previously (7). The docking model suggests why the *T. maritima* enzyme may not be able to accommodate D-Asp residues. The carbonyl oxygen of the D-Asp is positioned to potentially clash (2.4 Å) with the CG2 atom in Val-45 from the *T. maritima* structure but not with any residues in the human or *P. furiosus* enzymes. *c*, the polymorphic site at residue 119. The exposed side chain of Val-119 is in a position such that the other polymorph (Ile-119) would probably form a hydrophobic interaction with Leu-130, which might increase the stability of the protein. Val-119 and Leu-130 are shown in Corey-Pauling-Koltun models. The leucine is located in a short α-helix, which is not seen in the other structures of PIMT.

ices and one C-terminal α-helix. It has been reported that the bovine enzyme contains a disulfide bond linking Cys-42 to Cys-94 (29). In the structure reported here, those residues are 20 Å apart, suggesting that no disulfide bond exists in the native enzyme, and that the formation of such a disulfide may occur during the processing of tryptic peptides for analysis.

Comparison with Other PIMT Structures—The structure of human PIMT is shown in the same orientation in Fig. 1*B* along with the aligned PIMT structures from *T. maritima* (1DL5) and *P. furiosus* (1JG3) with root mean square differences for the aligned C-α atoms of 1.4 and 0.9 Å, respectively. There are a few notable features that distinguish the human PIMT struc-

ture from those structures reported recently from other organisms. In the human enzyme, the C-terminal part of the chain takes a different course. Also in the human enzyme, the loop following α-helix B contains a short α-helix not found in the two previously reported structures (Fig. 2*C*). Additional minor variations are apparent in the loop regions before and after β-strand 6.

Electrostatic Effects of Buried Charges Near the Active Site—An inspection of the crystal structure surprisingly revealed three charged amino acid residues (Asp-83, Arg-36, and Asp-109) essentially buried in the protein interior. Buried charges are relatively rare because of the energetic cost of desolvating a charge and moving it into the protein interior where the dielectric value is much lower than it is in the aqueous solvent. When buried charges do occur, the low dielectric value can produce significant electrostatic effects. The occurrence in this enzyme of three buried charges seems especially unusual. These charged residues are also relatively well conserved across the PIMT family of enzymes, further implicating them in some functional role. Although the charged residues are also present in the other two recently reported PIMT structures (Asp-97, Arg-48, and Glu-121 in *P. furiosus* and Glu-81, Arg-27, and Glu-107 in *T. maritima*), the electrostatic effects of these residues were not discussed in earlier analyses.

The buried protein charges are especially interesting in view of the charged nature of the reactive groups; the cofactor bears a sulfonium, and the polypeptide substrates bear an attacking carboxylate. It may also be relevant that the reaction is accompanied by a neutralization of the charges on both reactive groups. Because all three buried charges lie in the vicinity of the active site and the cofactor binding site, they might make important contributions to the energetics of binding or catalysis.

The electrostatic potential was calculated (see "Experimental Procedures") and examined in detail at the positions that would be occupied by the sulfonium and the isoaspartyl substrate carboxylate in a productive complex. The contributions to the electrostatic potential were included from the protein as well as from charged groups on the AdoMet cofactor excluding the sulfonium charge itself. The protein charge closest to the reactive groups is Asp-109 (5.6 Å). As a result, the protein makes a significant net negative contribution to the potential experienced by the charged reactive groups in the active site. In units of k_BT per elementary charge, the protein produces a very high electrostatic potential of $-18\ k_BT$ at the sulfonium and $-6\ k_BT$ at the carboxylate.

Mutagenesis experiments could help clarify the possible roles of buried charges in binding and catalysis, but the electrostatic calculations already provide some clues. It is noteworthy that the electrostatic potential difference at the two reactive charged groups does not appear to specifically promote the chemical step (methyl transfer). In fact, such an electrostatic driving force would probably be unproductive at this point in the reaction mechanism, because the reaction is energetically favorable as it is even in the unbound state. Rather, the electrostatic contributions from the protein may be serving to help bind the charged AdoMet form of the cofactor by partially compensating for the significantly unfavorable energy associated with binding and desolvating its charged sulfonium in the buried active site cleft. Given the extraordinary burial of the cofactor, it seems likely that the rate-limiting steps in the reaction cycle could involve cofactor binding or release. The strong electrostatic interactions between buried charges on the protein and the cofactor could play important roles in those steps of the reaction cycle.

Role of Proline 45 in Substrate Specificity—A proline residue conserved in the active site of archael and eucaryotic enzymes may explain the ability of these enzymes to catalyze methylation of D-Asp more readily than the eubacterial enzymes. One of the recently reported structures (7) from *P. furiosus* was determined in the presence of a polypeptide substrate, VYP(L-isoAsp)HA. This structural complex provides a framework for understanding the substrate specificities of the enzymes from various sources. L-IsoAsp residues can be methylated by PIMT from all three organisms, whereas the D-Asp amino acid can be methylated by PIMT from human and *P. furiosus* (8) but not from *T. maritima* (5). PIMT from human and *P. furiosus* both have a proline in a key position (Pro-49/Pro-65) at which PIMT from *T. maritima* is replaced by a valine (Val-45). When the structure of the L-isoAsp polypeptide substrate visualized in the *P. furious* structure is overlaid onto the other two protein structures, no steric clashes are seen with either the human or the *T. maritima* enzyme (Fig. 2*A*). Contrasting results are obtained when a similar analysis is performed with a D-Asp-containing polypeptide, which was modeled earlier on the basis of the L-isoAsp structure (7). The analysis suggests that the carbonyl group of the D-Asp would clash with CG2 in Val-45 in the structure from *T. maritima* (Fig. 2*B*) but not with the equivalently positioned proline in human and *P. furiosus.* The idea that residue 45 plays a key role in substrate specificity could be tested by mutagenesis. Counter to this argument, a proline residue is present in the nematode enzyme, which does not recognize D-aspartyl residues. Thus, other factors may also be important for the ability of the human and *P. furiosus* enzymes to recognize D-aspartyl residues with high efficiency.

Polymorphism—Because of a genetic polymorphism in Caucasian populations, two alternate alleles of the isoaspartyl methyltransferase *PCMT1* gene (on chromosome 6) lead to the production of enzymes containing either a valine or isoleucine residue at position 119 (12). The presence of the isoleucine residue is associated with increased thermal stability of the enzyme, whereas the presence of the valine residue is associated with higher apparent affinity for protein, but not peptide, methyl-accepting substrates (12). In the human methyltransferase structure reported here, Val-119 is found to be almost completely exposed. The residue is located on the opposite side of the molecule from the methylation active site, so it is not immediately clear how the change from a valine to an isoleucine residue can affect the affinity for protein substrates. However, the larger isoleucine residue would be expected to form a hydrophobic interaction with Leu-130 located in α-helix 7 and might thereby increase the stability of the protein (Fig. 2*C*).

In addition to the genetic polymorphism, an alternative splicing of the human *PCMT1* gene transcript in most tissues leads to two electrophoretic variants of the enzyme (10, 11). These products differ at the C terminus by the presence of WK or DEL as the terminal amino acid sequence. In the structure seen here, clear electron density is not observed for the C-terminal residues after 224, and it appears that these residues probably project from the enzyme surface.

Acknowledgments—We thank the staff of the Brookhaven National Laboratory beamline X8C.

REFERENCES

1. Young, A. L., Carter, W. G., Doyle, H. A., Mamula, M. J., and Aswad, D. W. (2001) *J. Biol. Chem.* **276,** 37161–37165
2. Ingrosso, D., D'Angelo, S., di Carlo, E., Perna, A. F., Zappia, V., and Galletti, P. (2000) *Eur. J. Biochem.* **267,** 4397–4405
3. Chavous, D. A., Jackson, F. R., and O'Connor, C. M. (2001) *Proc. Natl. Acad. Sci. U. S. A.* **98,** 14814–14818
4. Kagan, R. M., McFadden, H. J., McFadden, P. N., O'Connor, C., and Clarke, S. (1997) *Comp. Biochem. Physiol.* **117,** 379–385
5. Ichikawa, J. K., and Clarke, S. (1998) *Arch. Biochem. Biophys.* **358,** 222–231
6. Skinner, M. M., Puvathingal, J. M., Walter, R. L., and Friedman, A. M. (2000) *Structure Fold Des.* **8,** 1189–1201

7. Griffith, S. C., Sawaya, M. R., Boutz, D. R., Thapar, N., Katz, J. E., Clarke, S., and Yeates, T. O. (2001) *J. Mol. Biol.* **313,** 1103–1116
8. Thapar, N., Griffith, S. C., Yeates, T. O., and Clarke, S. (2002) *J. Biol. Chem.* **277,** 1058–1065
9. Thapar, N., and Clarke, S. (2000) *Protein Expression Purif.* **20,** 237–251
10. MacLaren, D. C., Kagan, R. M., and Clarke, S. (1992) *Biochem. Biophys. Res. Commun.* **185,** 277–283
11. Potter, S. M., Johnson, B. A., Henschen, A., Aswad, D. W., and Guzzetta, A. W. (1992) *Biochemistry* **31,** 6339–6347
12. DeVry, C. G., and Clarke, S. (1999) *J. Hum. Genet.* **44,** 275–288
13. Maclaren, D. C., and Clarke, S. (1995) *Protein Expression Purif.* **6,** 99–108
14. Redinbo, M. (1995) *Structural Studies of Plastocyanin and Human Amyloid β-peptide*, Ph.D. thesis, University of California, Los Angeles
15. Smith, C. D., Barchue, J., Mentel, C., DeLucas, L., Shirasawa, T., and Chattopadhyay, D. (1997) *Proteins* **28,** 457–460
16. Griffith, S. (2002) *Crystal Structure of a Protein Repair Methyltransferase from Pyrococcus furiosus with its L-Isoaspartyl Peptide Substrate*, Ph.D. thesis, University of California, Los Angeles
17. Otwinowski, Z., and Minor, W. (1997) *Methods Enzymol.* **27,** 307–326
18. Kissinger, C. R., Gehlhaar, D. K., and Fogel, D. B. (1999) *Acta Crystallogr. Sec. D* **55,** 484–491
19. Jones, T. A., Zou, J. Y., Cowan, S. W., and Kjeldgaard, T. (1991) *Acta Crystallogr. Sec. A* **47,** 110–119
20. Brunger, A. T., Adams, P. D., Clore, G. M., DeLano, W. L., Gros, P., Grosse-Kunstleve, R. W., Jiang, J. S., Kuszewski, J., Niges, M., Pannu, N. S., Read, R. J., Rice, L. M., Simonson, T., and Warren, G. L. (1998) *Acta Crystallogr. Sec. D* **54,** 905–921
21. Laskowski, R. A., Moss, D. S., and Thornton, J. M. (1993) *J. Mol. Biol.* **231,** 1049–1067
22. Colovos, C., and Yeates, T. O. (1993) *Protein Sci.* **2,** 1511–1519
23. Warwicker, J., and Watson, H. C. (1982) *J. Mol. Biol.* **157,** 671–679
24. Yeates, T. O., Komiya, H., Rees, D. C., Allen, J. P., and Feher, G. (1987) *Proc. Natl. Acad. Sci. U. S. A.* **84,** 6438–6442
25. Nicholls, A., Sharp, K. A., and Honig, B. (1991) *Proteins* **11,** 281–296
26. Press, W. H., Teukolsky, S. A., Vettering, W. T., and Flannery, B. P. (1986) *Numerical Recipes*, Cambridge University Press, Cambridge, UK
27. Schluckebier, G., O'Gara, M., Saenger, W., and Cheng, X. (1995) *J. Mol. Biol.* **247,** 16–20
28. Fauman, E. B., Blumenthal, R. M., and Cheng, X. (1999) in *S-Adenosylmethionine-dependent Methyltransferases: Structures and Functions* (Cheng, X., and Blumenthal, R. M., eds), pp. 1–38, World Scientific, River Edge, NJ
29. Henzel, W. J., Stults, J. T., Hsu, C. A., and Aswad, D. W. (1989) *J. Biol. Chem.* **264,** 15905–15911
30. Kraulis, P. J. (1991) *J. Appl. Crystallogr.* **24,** 946–950
31. Merrit, E. A., and Murphy, M. E. P. (1994) *Acta Crystallogr. Sec. D* **50,** 869–873